Neural adaptive control by state space system UPFC (SSNN) for compensation of active And reactive power

Bouanane Abdelkrim, Chaker Abdelkader, Addadi Zoubida, Amara Mohamed

Abstract—in our present paper, we present the effectiveness of the controller's electrical power flow Universal (unified power flow controller UPFC) with the choice of a control strategy. To evaluate the performance and robustness of the system, we proposed a hybrid control combining the concept of neural networks with conventional regulators vis-à-vis the changes in characteristics of the transmission line in order to improve the stability of the electrical power network.

Index Terms—UPFC system, adaptive control, neural networks, state space (SSNN).

1 Introduction

With the rapid development of the modern world, the demand for electricity is growing and electrical installations are continually enhanced to meet these requirements. The construction of new plants and new lines are necessary, but with FACTS devices, we can solve some problems while using the existing facilities.

Having highlighted the need for rapid control of power flow in transmission line and the description of the new concept of "FACTS" that was born to meet the increasing difficulties in networks including control of the flow on the axes transport, we are interested in our work to the controller's electrical power flow universal [1], [2] (Unified Power Flow Controller UPFC).

The UPFC consists of two switching converter, (series and shunt) (Fig. 1) and even this device is the union of a parallel compensator and a series compensator. It is capable of simultaneously and independently control the active power and reactive power. It can control the three parameters associated with power flow the line voltage, the impedance of the line and angle of transport.

2 Configuration Variable Universal Charges (UPFC):

It is assumed that the UPFC [3] shown in Fig. 1 was plugged into a simplified transmission system, the arrival of the transmission line (Receiving End). The two voltage source inverters constituting the UPFC are connected together through a common DC circuit.
Two transformers T1 and T2 are used to connect the two inverters, one serial and one parallel to the transmission line.

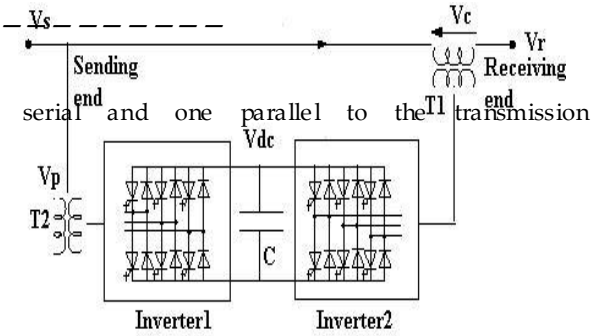

Fig. 1 UPFC System Configuration

After all, this composition offers the UPFC's ability to control the active power and reactive power regardless of where:
- The series inverter (2) "Inverter2" performs the principal function of the UPFC by injecting an AC voltage in series (AC) with an amplitude and a phase angle adjustable.
- The parallel UPS (1) "Inverter1 'role is to provide or absorb the real power demanded by the inverter (2) to the connection (DC), as it can also produce or absorb reactive power according to demand, and provide independent shunt compensation transmission line.
The series inverter (2) provides or absorbs the needed reactive power locally produced active power as a result of injecting a voltage in series.

3 Modelling Of the System UPFC:

The simplified circuit of the control system and compensation of UPFC is shown in (Fig. 2) modeling of this circuit is based on simplifying assumptions in the form of ideal voltage sources then the dynamic equations of the UPFC are divided into three systems of equations: the equations of the series branch, the equations of parallel branch and those of the DC

Bouanane,, Addadi and Amara are teachers in the department of electrical engineering at the University Dr. MOULAY TAHER, in SAIDA, Algeria. (bouananeabd@yahoo.fr)
Chaker is professor in the department of electrical engineering at the ENSET in ORAN, Algeria. (chakeraa@yahoo.fr)

circuit.

By applying Kirchhoff's laws we will have the following equations.

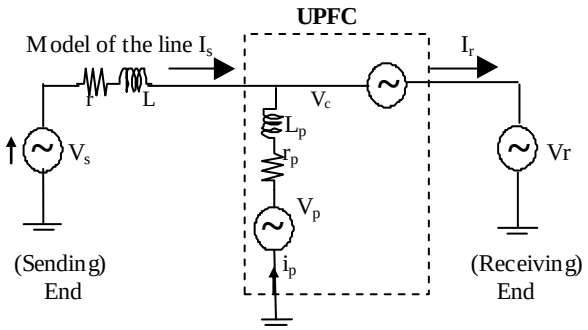

Fig. 2 Equivalent circuit of UPFC

3.1 The modelling of the UPFC series branch:

The mathematical model is given by the following equations:

$$\frac{di_{sa}}{dt} = -\frac{r}{L}.i_{sa} + \frac{1}{L}\left(v_{sa} - v_{ca} - v_{ra}\right)$$
$$\frac{di_{sb}}{dt} = -\frac{r}{L}.i_{sb} + \frac{1}{L}.\left(v_{sb} - v_{cb} - v_{rb}\right) \quad (1)$$
$$\frac{di_{sc}}{dt} = -\frac{r}{L}.i_{sc} + \frac{1}{L}.\left(v_{sc} - v_{cc} - v_{rc}\right)$$

The transformation of Park aims to model this three-phase system (a, b, c) two-phase (d, q) as follows: (2)

$$\begin{bmatrix} x_d \\ x_q \\ x_o \end{bmatrix} = \frac{2}{3}\begin{bmatrix} \cos(\omega t) & -\sin(\omega t) & 1/2 \\ \cos(\omega t - 120°) & -\sin(\omega t - 120°) & 1/2 \\ \cos(\omega t + 120°) & -\sin(\omega t + 120°) & 1/2 \end{bmatrix}^T \begin{bmatrix} x_a \\ x_b \\ x_c \end{bmatrix}$$

Where x; can be a voltage or current.

In our case, the component x0 is not seen as the power system is assumed to be symmetric. After the transformation of Park, equation (1) is expressed in the d_q reference by the equations:

$$\frac{di_{sd}}{dt} = \omega.i_{sq} - \frac{r}{L}.i_{sd} + \frac{1}{L}\left(v_{sd} - v_{cd} - v_{rd}\right)$$
$$\frac{di_{sq}}{dt} = -\omega.i_{sd} - \frac{r}{L}.i_{sq} + \frac{1}{L}\left(v_{sq} - v_{cq} - v_{rq}\right) \quad (3)$$

The matrix form of the dq axis can be rewritten as follows:

$$\frac{d}{dt}\begin{bmatrix} i_{sd} \\ i_{sq} \end{bmatrix} = \begin{bmatrix} -r/l & +\omega \\ -\omega & -r/l \end{bmatrix}.\begin{bmatrix} i_{sd} \\ i_{sq} \end{bmatrix} + \frac{1}{l}.\begin{bmatrix} v_{sd} - & v_{cd} - & v_{rd} \\ v_{sq} - & v_{cq} - & v_{rq} \end{bmatrix}$$

3.2 The modelling of the shunt branch:

The mathematical model of the UPFC shunt is given similarly by the following equations:

$$\frac{di_{pa}}{dt} = -\frac{r_p}{L_p}.i_{pa} + \frac{1}{L_p}.\left(v_{pa} - v_{ca} - v_{ra}\right)$$
$$\frac{di_{pb}}{dt} = -\frac{r_p}{L_p}.i_{pb} + \frac{1}{L_p}.\left(v_{pb} - v_{cb} - v_{rb}\right) \quad (4)$$
$$\frac{di_{pc}}{dt} = -\frac{r_p}{L_p}.i_{pc} + \frac{1}{L_p}.\left(v_{pc} - v_{cc} - v_{rc}\right)$$

With a transformation marker d, q we have the system of equations (5):

$$\frac{di_{pd}}{dt} = \omega.i_{pq} - \frac{r_p}{L_p}.i_{pd} + \frac{1}{L_p}\left(v_{pd} - v_{cd} - v_{rd}\right)$$
$$\frac{di_{pq}}{dt} = -\omega.i_{pd} - \frac{r_p}{L_p}.i_{pq} + \frac{1}{L_p}\left(v_{pq} - v_{cq} - v_{rq}\right) \quad (5)$$

The matrix form is given as follows:

$$\frac{d}{dt}\begin{bmatrix} i_{pd} \\ i_{pq} \end{bmatrix} = \begin{bmatrix} -r_p/l_p & -\omega \\ -\omega & -r_p/l_p \end{bmatrix}.\begin{bmatrix} i_{pd} \\ i_{pq} \end{bmatrix} + \frac{1}{l}.\begin{bmatrix} v_{sd} - & v_{cd} - & v_{rd} \\ v_{sq} - & v_{cq} - & v_{rq} \end{bmatrix}$$

3.3 The modelling of the UPFC continues branch:

By passing on the principle of balance of power and neglecting the losses of the converters. The DC voltage V_{dc} by the following equation:

$$\frac{dv_c}{dt} = \frac{1}{C v_c}\left(p_e - p_{ep}\right) \quad (6)$$

Hence $p_e = v_{ca}\, i_{sa} + v_{cb}\, i_{sb} + v_{cc} i_{sc}$

$p_{ep} = v_{pa}\, i_{pa} + v_{pb}\, i_{pb} + v_{pc} i_{pc}$

With: p_e: active power consumption of the AC system

Pep: active power injected by the shunt inverter AC system

Applying the Park transformation on equation (6) we obtain:

$$\frac{dv_{dc}}{dt} = \frac{3}{2\,C\,v_{dc}}\left(v_{pd}\, i_{pd} + v_{pq}\, i_{pq} - v_{cd}\, i_d - v_{cq}\, i_q\right) \quad (7)$$

The UPFC series and shunt UPFC's are identical in every respect. The commands used to set the inverter are the same for the shunt inverter.

4 Configuration Control Circuit:

Theoretically the UPFC should be treated as a multivariable system because both series and shunt converters are connected from one side to the transmission line and the other side in continuous DC circuit and thus each has two inputs and two outputs. This for to facilitate the synthesis of settings, treatment of the two converters will be done separately. The possibility of this separation is justified by two main factors. First, the coupling between the two converters of the transmission line is quite small. Second, the dynamic variation of the voltage of DC side of the continuum is dominated by the parallel converter. Control of the converter in parallel UPFC is very similar to that of the compensator SVC. So to control the flow of active power in the transmission line, the controller of the UPFC series must adjust the angle of the phase of the compensation voltage V_c while to adjust the flow of reactive power, the amplitude of the input voltage range must be controlled. To ensure system stability, a chain of control is implemented with PI control.

- Control of the series branch
- Control of parallel branch and the game continues.

4.1 Description of the Control System of UPFC:

The active and reactive powers P and Q are given by the equations: $P=\frac{3}{2}\left(V_{sd}.i_{sd}+V_{sq}.i_{sq}\right)$ $Q=\frac{3}{2}\left(V_{sd}.i_{sq}-V_{sq}.i_{sd}\right)$ (8)

Where $i_{rd}=i_{sd}+i_{pd}$

$i_{rq}=i_{sq}+i_{pq}$

The reference power and reactive P * and Q * of the desired real powers P and Q are used as input to the control system of UPFC. From equation (8) the reference currents i_{sd} * and i_{sq} * can be calculated as follows:

$$i_q^*=\frac{2}{3}\left(\frac{P^*.V_{sq}+Q^*.V_{sd}}{\Delta}\right) \quad i_q^*=\frac{2}{3}\left(\frac{P^*.V_{sq}+Q^*.V_{sd}}{\Delta}\right) \qquad (9)$$

With $\Delta=V_{sd}^2+V_{sq}^2$

The reference power and reactive P * and Q * of the desired real powers P and Q are used as input to the control system of UPFC. From equation (8) the reference currents i_{sd}*and i_{sq}* can be calculated as follows. The reference currents I_{rdref} I_{rqref} and are calculated according to equations (8). These reference values and I_{rdref} I_{rqref} are then compared with actual line currents from the receiver.

The outputs of the PI editors provide the current values of control voltages V_{sd} and V_{cq}. The goal is to have active and reactive power at the finish line (Receiving End) identical to those instructions (P *, Q *) by forcing the line currents (I_{sd}, I_{sq}) to monitor properly their references. The reference currents calculated (8) compared to the actual line currents and after a correction to the current one ends control voltages (UPFC series) and V_{cd} V_{cq} representing the reference voltage control circuit (PWM) of the inverter in Fig. 3.

4.2 Decoupled PI Controller

According to the system of equations (3) or (5), one can have the system contains a coupling between the reactive and active current Id Iq. The interaction between current loops caused by the coupling term (ω) (Fig. 3). This explains the deviation of reactive power with respect to the reference. To reduce the interaction between the active and reactive power, a decoupling of the two current loops is needed.The function of decoupling is to remove the product ωL and I_q controller along the axis d and adding the product term ωL I_d and the controller along the axis q. The design of the control system must begin with the selection of variables to adjust and then that of the control variables and their association with variables set. There is various adjustment techniques well suited to the PI controller. There are two well-known empirical approaches proposed by Ziegler and Tit for determining the optimal parameters of the PI controller. The method Ziegler-Nichols, used in the present thesis is based on a trial conducted in closed loop with a simple analog proportional controller. The gain Kp of the regulator is gradually increased until the stability limit, which is characterized by a steady oscillation. Based on the results obtained, the parameters of the PI controller given by the analog transfer function.

$$K(s)=K_p\left(1+\frac{1}{T_i\,s}\right)$$

We can say in the conditions of the converter, the excess currents should be minimal. Therefore, the introduction of a simple condition $K_i=(r/L).k_p$. We obtain the transfer function $F(s)=k_p/k_p+s$ of the form is first class with a time constant $T=1/k_p$ .Hence

$$F(s)=\frac{1}{1+s.T} \qquad (10)$$

Thus, determining the time constant depends on the maximum allowable change of control variables and V_{cd} V_{cq} for controller series and the same for the shunt converter. So according to the method of Ziegler-Nichols, the critical gain K_{pc} and the period T_c of the oscillations is measured by the choice of the table as follows:

K_p =0,45 k_{pc} et T_i =0,83 T_c avec T_d=0

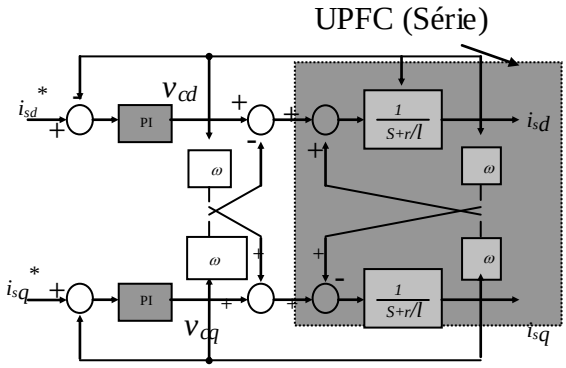

Fig. 3 Block Diagram of the UPFC Control (series)

4.2 Simulation Results with PI-D UPFC:

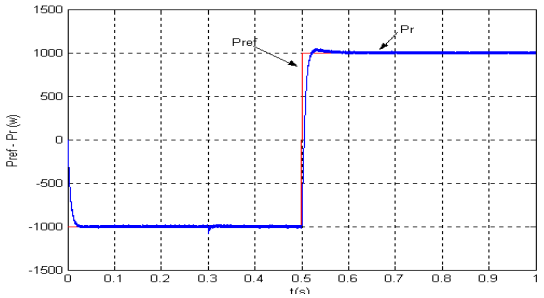

(a)

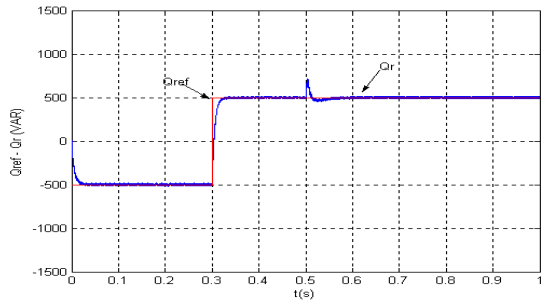

(b)

Fig. 4 (a), (b). Answers of Powers with PI-D.

Figures (4-a, b) illustrates the behaviour of active and reactive power, where we see that the control system has a fast dynamic response to the forces reach their steady states after a change in the reference values.

We also note the presence of the interaction between the two components (d and q). These influences are caused by the PWM inverter is unable to produce continuous signals needed by the decoupling, thus increasing the error in the PI-D controllers.

To test robustness, we tested for a variation of the reactance XL to 30% and I had variations on the output power following

Following these changes, the active and reactive power (Fig. 5) undergo large deviations more or less with an overflow at times of great change instructions (Pref, Qref), which means the performance degradation of the PI controller, interpreted by the loss of system stability

We simulated this time by introducing perturbation (Fig. 6) duration of 25 ms and amplitude 1.5 to test again its robustness and stability of the system.

The response of active and reactive power at 30% of XI could be detected; the error message given by "MATLAB command" indicated the saturation of the order at infinity in the spikes of the reference signals.

We can check the response of the servo not only continued but also regulation by adding a disturbance

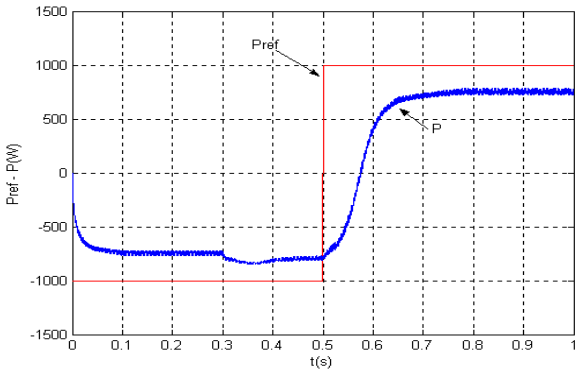

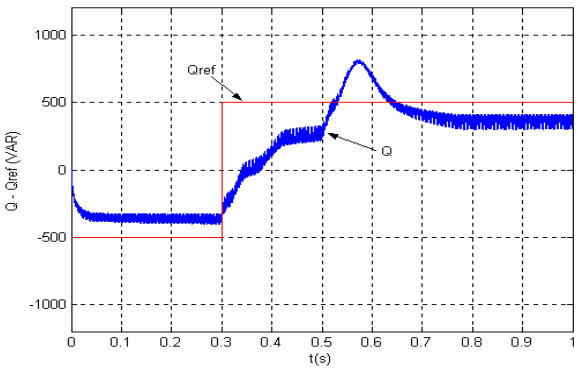

Fig. 5 Answers Powers to Change the Reactance of 30%

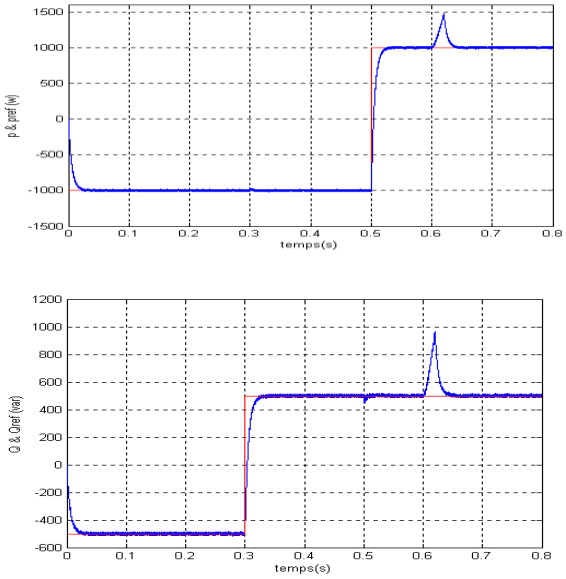

Fig.6. UPFC System Perturbed to Test Stability

5 Adaptive Neural Controls:

The interest in adaptive control [4] appears mainly at the level of parametric perturbations, ie act on the characteristics of the process to be controlled, disturbance acting on the variables to control or order. In this paper we present the method of adjustment proposed for the UPFC, emphasizing the classical approach based on neural networks.

5.1Choix a Neural Network:

In this paper the Elman network [5] said hidden layer network is a recurrent network, and therefore better suited for modelling dynamic systems. His choice in the neural control by state space is justified by the fact that, in particular, the network can be interpreted as a state space model nonlinear. Learning by back propagation algorithm standard is the law used for the identification of the UPFC.

5.2State Space Adaptive Neural Control« SSNN»:

The integration of these two approaches (neural adaptive control) [6] in a single hybrid structure, that each benefits from the other, but to change the dynamic behaviour of the UPFC system was added against a reaction calculated from the state vector (state space) (Fig. 7).

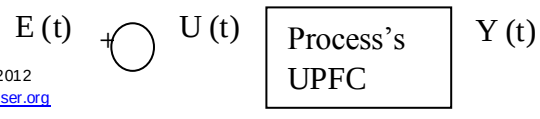

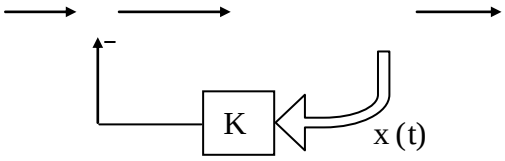

Fig. 7 Block Diagram of Feedback Control State of the UPFC.

The state feedback control is to consider the process model in the form of an equation of state:

$$X^{*}(t) = A\,x(t) + B\,u(t) \quad (11)$$

And observation equation:

$$Y(t) = C\,x(t) + D\,u(t) \quad (12)$$

Where u(t) is the control vector, x (t) the state vector, and y (t) the output vector of dimension for a discrete system to the sampling process parameters Te at times of Te sample k are formalized as follows :

$$x(t+1) = A_d\,x(t) + B\,u_d(t) \quad (14)$$

$$Y(t) = C_d\,x(t) + D_d\,u(t) \quad (15)$$

The transfer function G (s) = Y (s) / U (s) of our process UPFC can be written as:

$$G(s) = \frac{1}{s + r/L} \quad (16)$$

We deduce the equations of state representation of the UPFC:

$$\begin{cases} x^{*} = -\left(\frac{r}{L}\right).x + u \\ y = x \end{cases} \quad (17)$$

With: $U(t) = e(t) - k\,x(t)$

Let: $X(t+1) = [A_d - K B_d]\,x(t) + B_d\,e(t)$ (18)

$$Y(t) = C_d\,x(t) \quad (19)$$

The dynamics of the process corrected by state space is presented based on the characteristic equation of the matrix $[A_d - B_d K]$, where K is the matrix state space controlled process.

Our system is described in matrix form in the state space:

$$\begin{cases} x^{*} = A.x + B.u \\ y = C.x + D.u \end{cases} \quad (20)$$

Where:

$$A = \begin{bmatrix} \frac{-r}{L} & \omega \\ -\omega & \frac{-r}{L} \end{bmatrix} \quad B = \begin{bmatrix} \frac{-1}{L} & 0 \\ 0 & \frac{-1}{L} \end{bmatrix} \quad C = \begin{bmatrix} 1 & 0 \\ 0 & 1 \end{bmatrix} \quad D = \begin{bmatrix} 0 & 0 \\ 0 & 0 \end{bmatrix}$$

$$u = \begin{bmatrix} v_{cd} \\ v_{cq} \end{bmatrix} \quad y = \begin{bmatrix} i_{sd} \\ i_{sq} \end{bmatrix} \quad x = \begin{bmatrix} i_{sd} & i_{sq} \end{bmatrix}^{T}$$

5.3 Identification Based Network Elman:

Process identified [7] [8] will be characterized by the model structure (Fig. 8), of his order and parameter values. It is therefore, a corollary of the simulation process for which using a model and a set of coefficients to predict the response of the system. The Elman network consists of three layers: an input layer, hidden layer and output layer. The layers of input and output interfere with the external environment, which is not the case for the intermediate layer called hidden layer ie the network input is the command U (t) and its output is Y (t).

The state vector X (t) from the hidden layer is injected into the input layer.

We deduce the following equations:

$$X(t) = W_r\,X(t-1) + W_h\,U(t-1) \quad (21)$$

$$Y(t) = W_o\,X(t) \quad (22)$$

Where, Wh ; Wr et Wo are the weight matrices. Equations are standard descriptions of the state space of dynamical systems. The order of the system depends on the number of states equals the number of hidden layers. When an input-output data is presented to the network at iteration k squared error at the output of the network is defined as

$$E_t = \frac{1}{2}\left(y_d(t) - y(t)\right)^2 \quad (23)$$

For all data u (t), y_d (t) de t = 1,2,….. N, the sum of squared errors is:

$$E = \sum_{t=1}^{N} E_t \quad (24)$$

The weights are modified at each iteration, for W_0 we have:

$$\frac{\partial E_t}{\partial W_0} = -\left(y_d(t) - y(t)\right)\frac{\partial y(t)}{\partial W_0} = -\left(y_d(t) - y(t)\right)x^{T}(t) \quad (25)$$

For Wh et Wr, were:

$$\frac{\partial E_t}{\partial W_h} = -\frac{\partial E_t}{\partial y(t)}.\frac{\partial y(t)}{\partial x(t)}.\frac{\partial x(t)}{\partial W_h} = -\left(y_d(t) - y(t)\right)W_0^{T}.u(t) \quad (26)$$

$$\frac{\partial E_t}{\partial W_r^{i}} = -\frac{\partial E_t}{\partial y(t)}.\frac{\partial y(t)}{\partial x_i(t)}.\frac{\partial x_i(t)}{\partial W_r^{i}} = -\left(y_d(t) - y(t)\right)W_0^{i}\frac{\partial x_i(t)}{\partial W_r^{i}} \quad (27)$$

The latter we obtain:

$$\frac{\partial x_i}{\partial W_r^{i}} = X^{T}(t-1) + W_r^{i}.\frac{\partial x(t-1)}{\partial W_r^{i}} \quad (28)$$

The variation of the weight matrix based on the learning gain is written as:

$$\Delta W = -\eta.\frac{\partial E_t}{\partial W} \quad (29)$$

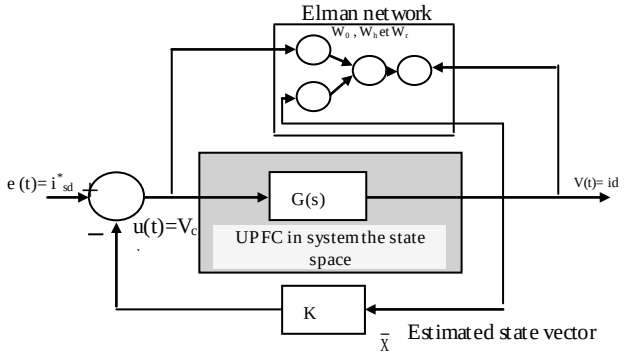

Fig. 8 Network ELMAN and State Space.

Note that the performance of the identification is better when the input signal is sufficiently high in frequency to excite the different

modes of process. The three weights Wo, Wr and Wh which are respectively the matrices of the equation of state of the process system (UPFC) [CA and B] became stable after a rough time t = 0.3s and several iterations (fig. 9).

Note: For the Elman network neuron type is assumed through the vector is zero (D = 0).

In online learning Elman network, the task of identifying and correcting same synthesis are one after the other. Or correction of the numerical values of the parameters is done repeatedly so the estimation error (Fig. 10) takes about almost a second (t = 1s) to converge to zero i.e regulation in pursuit.

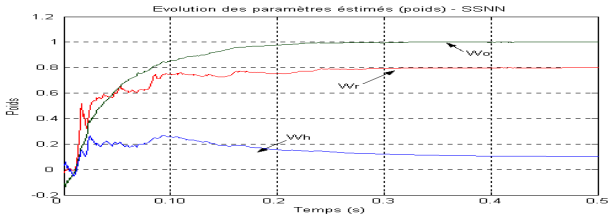

Fig. 9 Changing Weight

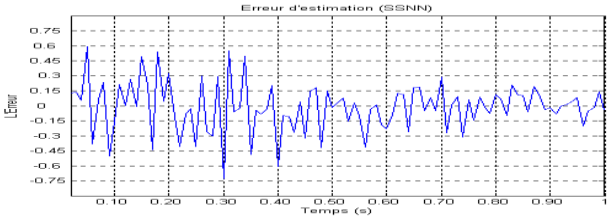

Fig. 10 Estimation Error

5.4 Robustness Test:

To check the robustness to the controller, two tests were performed. For each test we varied the parameters of the transmission line but the controller remains unchanged. It can be seen that the variation of the reactance (± 25%) has almost no influence on the output characteristics of the UPFC system (Fig. 11).To compare the responses of active and reactive power of UPFC system, we gave the three cases (Fig. 11) Where (a) and (c) are the responses to changes (± 25%) and (b) is the response of the system without any change in reactance.

(a)

(b)

(c)

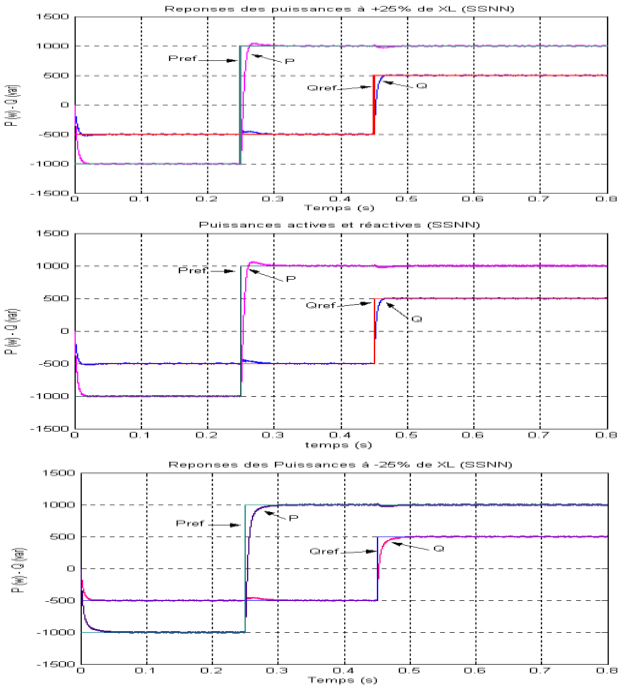

Fig. 11 Neural Adaptive Control (SSNN) Powers P, Q And at (± 25% XL)

6 Conclusion

The identification process will be characterized by the model structure, its order and parameter values. It is therefore a corollary of the simulation process which uses a model and a set of coefficients to predict the response of the system. The use of more advanced low-identification neural network can be dependable in the calculation algorithm of the order.

In this paper we used for the identification of system parameters a neuron network said Elman network with three layers. As we have already seen. Note that the performance of the identification is better when the input signal is sufficiently high in frequency to excite the different modes of process.

Neural adaptive control by state feedback (SSNN: state space neural network)) is a hybrid control based on the representation of system status UPFC was tested. The performance of the latter are slightly degraded, this is may be due to the delay caused by the algorithm, it can't be reduced at will, or it may due to the choice of the gain K of the closed loop.

Finally, the identification process based on learning of Elman neural network, provides the dynamic behavior of the process and to estimate the system output as its state vector based on the information that are control signal and the measured output.

7 References

[1] I. Papic, P. Zunko, D. Povh, M. Weinhold, "Basic control of unified power flow controller". *IEEE Trans. Power Syst.*, vol. 12, no. 4, pp. 1734–1739, 1997.

[2] Y. H. song and A .T. Johns,' flexible AC transmission systems (FACTS).' IEE power and Energy series 30.1999.

[3] Gyugyi L.: unified power flow control concept for flexible AC transmission systems. IEE Proc. 139 (1992) 323-331

[4] O. pages 'étude de comparaison de différentes structures de commande multi- contrôleurs application à un axe robotise.' thèse 2001. (LAMII/CESALP).université de Savoie.

[5] Xiang Li, Guanrong C., Zengqian C., and Z. Yuan 'Chaotifying Linear Elman Networks' IEEE transaction neural networks. vo1, 3.5 September 2002.

[6] M. A. Denaï, T. Allaoui, "Adaptive fuzzy Decoupling of UPFC-Power Flow Compensation", 37th UPEC2002, 9-11 September 2002, Straffordshires University UK.

[7] S. zebirate, A.chaker,O.traiaia , 'commande addaptative decouple neuronale d'un compensateur de flux de puissance UPFC'reference480.laboratoire LAAS.CCECE 03-CCGEI 2003.Montreal.IEEE May 2003.

[8] S. zebirate, A.chaker, 'commande addaptative decouple neuronale d'un UPFC (unified power flow control)', JCGE Saint Nazaire,Juin 2003.